A Multiresolution Tensor Spline Method for Fitting Functions on the Sphere

Tom Lyche [1] and Larry L. Schumaker [2]

Abstract. We present the details of a multi-resolution method which we proposed in Taormina in 1993 (see [6]) which is suitable for fitting functions or data on the sphere. The method is based on tensor products of polynomial splines and trigonometric splines, and produces surfaces which are tangent plane continuous. The result is a convenient compression algorithm for dealing with large amounts of data on the sphere. We give full details of a computer implementation which is highly efficient with respect to both storage and computational cost. We also demonstrate the performance of the method on two typical test examples.

Keywords: multiresolution, spherical data compression, tensor splines

§1. Introduction

In many applications (e.g., in geophysics, meteorology, medical modelling, etc.), one needs to construct smooth functions defined on the unit sphere S which approximate or interpolate data. As shown in [11], one way to do this is to work with tensor-product functions of the form

$$f(\theta,\phi) := \sum_{i=1}^{m}\sum_{j=1}^{\widetilde{m}} c_{ij}\varphi_i(\theta)\tilde{\varphi}_j(\phi) \tag{1.1}$$

defined on the rectangle

$$H := \{(\theta,\phi) : \ -\pi/2 \le \theta \le \pi/2 \ \text{ and } \ 0 \le \phi \le 2\pi\},$$

where the φ_i are quadratic polynomial B-splines on $[-\pi/2,\pi/2]$, and the $\tilde{\varphi}_j$ are periodic trigonometric splines of order three on $[0,2\pi]$. With some care in the choice of the coefficients (see Sect. 2), the associated *surface*

$$\mathcal{S}_f := \{f(\theta,\phi)\boldsymbol{v}(\theta,\phi) : \ (\theta,\phi) \in H\}$$

[1] Institutt for Informatikk, University of Oslo P.O.Box 1080, Blindern 0316 Oslo, Norway tom@ifi.uio.no. Supported by NATO Grant CRG951291. Part of the work was completed during a stay at "Institut National des Sciences Appliquées" and "Laboratoire Approximation et Optimisation" of "Université Paul Sabatier", Toulouse, France.

[2] Department of Mathematics, Vanderbilt University, Nashville, TN 37240, s@mars.cas.vanderbilt.edu. Supported by the National Science Foundation under grant DMS-9803340 and by NATO Grant CRG951291.

with $\boldsymbol{v}(\theta,\phi) = [\cos(\theta)\cos(\phi), \cos(\theta)\sin(\phi), \sin(\theta)]^T$ will be tangent plane continuous.

In practice we often encounter very large data sets, and to get good fits using tensor product splines (1.1), a large numbers of knots are required, resulting in many basis functions and many coefficients. Since two spline spaces are nested if their knot sequences are nested, one way to achieve a more efficient fit without sacrificing quality is to look for a multiresolution representation of (1.1), i.e., to recursively decompose it into splines on coarser meshes and corresponding correction (wavelet) terms. Then compression can be achieved in the standard way by thresholding out small coefficients.

The paper is organized as follows. In Sect. 2 we introduce notation and give details on the tensor product splines to be used here. In Sect. 3 we describe the general decomposition and reconstruction algorithm in matrix form, while in Sect. 4 we present a tensor version of the algorithms. The required matrices corresponding to the polynomial and trigonometric spline spaces, respectively, are derived in Sections 5 and 6. Sect. 7 is devoted to details of implementing the algorithm. In Sect. 8 we present test examples, and in Sect. 9 several concluding remarks.

§2. Tangent plane continuous tensor splines

Let $\varphi_1, \ldots, \varphi_m$ be the standard normalized quadratic B-splines associated with the knot sequence

$$-\pi/2 = x_1 = x_2 = x_3 < x_4 < \cdots < x_m < x_{m+1} = x_{m+2} = x_{m+3} = \pi/2.$$

Recall that φ_i is supported on the interval $[x_i, x_{i+3}]$, and that the B-splines form a partition of unity on $[-\pi/2, \pi/2]$. Let $T_1, \ldots, T_{\widetilde{m}}$ be the classical trigonometric B-splines of order 3 defined on the knot sequence $\tilde{x}_1, \ldots, \tilde{x}_{\widetilde{m}+3}$, where

$$0 = \tilde{x}_1 < \tilde{x}_2 < \cdots < \tilde{x}_{\widetilde{m}} < 2\pi,$$

and $\tilde{x}_{\tilde{m}+i} := \tilde{x}_i + 2\pi$, $i = 1, \ldots, 3$, see Sect. 6. Recall that T_j is supported on the interval $[\tilde{x}_j, \tilde{x}_{j+3}]$. Let

$$\tilde{\varphi}_j(x) = \begin{cases} T_j(x), & j = 1, \ldots, \widetilde{m}-2, \\ T_j(x) + T_j(x-2\pi), & j = \widetilde{m}-1, \widetilde{m}, \end{cases}$$

be the associated 2π-periodic trigonometric B-splines, see [10]. These splines can be normalized so that for $\phi \in [0, 2\pi]$

$$1 = \sum_{j=1}^{\widetilde{m}} \cos\big(\frac{\tilde{x}_{j+2} - \tilde{x}_{j+1}}{2}\big)\tilde{\varphi}_j(\phi) \tag{2.1}$$

$$\cos(\phi) = \sum_{j=1}^{\widetilde{m}} \cos\big(\frac{\tilde{x}_{j+1} + \tilde{x}_{j+2}}{2}\big)\tilde{\varphi}_j(\phi), \tag{2.2}$$

$$\sin(\phi) = \sum_{j=1}^{\widetilde{m}} \sin\big(\frac{\tilde{x}_{j+1} + \tilde{x}_{j+2}}{2}\big)\tilde{\varphi}_j(\phi). \tag{2.3}$$

Since the left and right boundaries of H map to the north and south poles, respectively, a function f of the form (1.1) will be well-defined on S if and only if

$$c_{1,j} = f_{\mathcal{S}} \cos\big(\frac{\tilde{x}_{j+2} - \tilde{x}_{j+1}}{2}\big), \quad j = 1, \ldots, \widetilde{m} \tag{2.4}$$

and

$$c_{m,j} = f_{\mathcal{N}} \cos\big(\frac{\tilde{x}_{j+2} - \tilde{x}_{j+1}}{2}\big), \quad j = 1, \ldots, \widetilde{m}, \tag{2.5}$$

where $f_{\mathcal{S}}$ and $f_{\mathcal{N}}$ are the values at the poles. Now since f is 2π-periodic in the ϕ variable and is C^1 continuous in both variables, we might expect that the corresponding surface $\mathcal{S}_f$ has a continuous tangent plane at nonpolar points. However, since we are working in a parametric setting, more is needed. The following theorem shows that under mild conditions on f which are normally satisfied in practice, we do get tangent plane continuity except at the poles.

Theorem 2.1. *Suppose f is a spline as in (1.1) which satisfies the conditions (2.4) and (2.5), and that in addition $f(\theta, \phi) > 0$ for all $(\theta, \phi) \in H$. Then the corresponding surface $\mathcal{S}_f$ is tangent plane continuous at all nonpolar points of S.*

Proof: Since f is a C^1 spline, the partial deriviatives f_θ and f_ϕ are continuous on H. Now $t_1(\theta, \phi) := D_\theta[f(\theta, \phi)\boldsymbol{v}(\theta, \phi)]$ and $t_2(\theta, \phi) := D_\phi[f(\theta, \phi)\boldsymbol{v}(\theta, \phi)]$ are two tangents to the surface $\mathcal{S}_f$ at the point $f(\theta, \phi)\boldsymbol{v}(\theta, \phi)$. The normal vector to the surface at this point is given by the cross product $\boldsymbol{n} := t_1 \times t_2$. By the hypotheses, $\boldsymbol{n}$ is continuous, and thus to assure a continuous tangent plane, it suffices to show that $\boldsymbol{n}$ has positive length (which insures that the surface does not have singular points or cusps). Using Mathematica, it is easy to see that

$$|\boldsymbol{n}(\theta, \phi)|^2 = f^2(\theta, \phi)\big[\cos(\theta)^2 f(\theta, \phi)^2 + f_\phi(\theta, \phi)^2 + \cos(\theta)^2 f_\theta(\theta, \phi)^2\big],$$

which is clearly positive for all values of $(\theta, \phi) \in H$ with $\theta \neq \pm\pi/2$. $\square$

With some additional side conditions on the coefficients of f, we can make the surface $\mathcal{S}_f$ also be tangent plane continuous at the poles. The required conditions (cf. [3,11]) are that

$$c_{2,j} = c_{1,j} + \frac{(x_4 - x_3)}{2}\big[A_{\mathcal{S}} \cos\big(\frac{\tilde{x}_{j+1} + \tilde{x}_{j+2}}{2}\big) + B_{\mathcal{S}} \sin\big(\frac{\tilde{x}_{j+1} + \tilde{x}_{j+2}}{2}\big)\big]$$

and

$$c_{m-1,j} = c_{m,j} - \frac{(x_{m+1} - x_m)}{2}\big[A_{\mathcal{N}} \cos\big(\frac{\tilde{x}_{j+1} + \tilde{x}_{j+2}}{2}\big) + B_{\mathcal{N}} \sin\big(\frac{\tilde{x}_{j+1} + \tilde{x}_{j+2}}{2}\big)\big]$$

for $j = 1, \ldots, \widetilde{m}$, where $A_{\mathcal{S}}$,$B_{\mathcal{S}}$,$A_{\mathcal{N}}$, and $B_{\mathcal{N}}$ are constants.

§3. Basic decomposition and reconstruction formulae

Suppose $\mathcal{V}_0, \mathcal{V}_1, \ldots$ are a nested sequence of finite-dimensional linear subspaces of an inner-product space X, i.e.

$$\mathcal{V}_0 \subset \mathcal{V}_1 \subset \cdots \subset \mathcal{V}_k \subset \cdots$$

Let

$$\mathcal{V}_k = \mathcal{V}_{k-1} \oplus \mathcal{W}_{k-1}$$

be the corresponding orthogonal decompositions.

For our application, it is convenient to express decomposition and reconstruction in matrix form, cf. [12]. Let $\varphi_{k,1}, \ldots, \varphi_{k,m_k}$ be a basis for $\mathcal{V}_k$, and let $\psi_{k-1,1}, \ldots, \psi_{k-1,n_{k-1}}$ be a basis for $\mathcal{W}_{k-1}$, where $n_{k-1} = m_k - m_{k-1}$. Then by the nestedness, there exists an $m_k \times m_{k-1}$ matrix P_k such that

$$\varphi_{k-1}^T = \varphi_k^T P_k, \tag{3.1}$$

where

$$\varphi_k = (\varphi_{k,1}, \ldots, \varphi_{k,m_k})^T.$$

The equation (3.1) is the usual *refinement relation*. Similarly, there exists an $m_k \times n_{k-1}$ matrix Q_k such that

$$\psi_{k-1}^T = \varphi_k^T Q_k, \tag{3.2}$$

where

$$\psi_{k-1} = (\psi_{k-1,1}, \ldots, \psi_{k-1,n_{k-1}})^T. \tag{3.3}$$

Let

$$\begin{aligned} G_k &= (\langle \varphi_{k,i}, \varphi_{k,j} \rangle) \\ H_{k-1} &= (\langle \psi_{k-1,i}, \psi_{k-1,j} \rangle) \end{aligned}$$

be the Gram matrices of size $m_k \times m_k$ and $n_{k-1} \times n_{k-1}$, respectively. It is easy to see that

$$H_{k-1} = Q_k^T G_k Q_k. \tag{3.4}$$

Clearly, the Gram matrices G_k and H_{k-1} are symmetric. The linear independence of the basis functions $\phi_{k,i}$ and of $\psi_{k,i}$ implies that both G_k and H_{k-1} are positive definite, and thus nonsingular.

The following lemma shows how to decompose and reconstruct functions in $\mathcal{V}_k$ in terms of functions in $\mathcal{V}_{k-1}$ and $\mathcal{W}_{k-1}$.

Lemma 3.1. *Let $f_k = \varphi_k^T a_k$ be a function in $\mathcal{V}_k$ associated with a coefficient vector $a_k \in \mathbb{R}^{m_k}$, and let*

$$f_k = f_{k-1} + g_{k-1} \tag{3.5}$$

be its orthogonal decomposition, where

$$f_{k-1} = \varphi_{k-1}^T a_{k-1} \in \mathcal{V}_{k-1}, \qquad g_{k-1} = \psi_{k-1}^T b_{k-1} \in \mathcal{W}_{k-1}.$$

Then

$$\begin{aligned} a_{k-1} &= G_{k-1}^{-1} P_k^T G_k a_k \\ b_{k-1} &= H_{k-1}^{-1} Q_k^T G_k a_k. \end{aligned}$$

Moreover,

$$a_k = P_k a_{k-1} + Q_k b_{k-1}. \tag{3.6}$$

Proof: To find a_{k-1}, we take the inner-product of both sides of (3.5) with $\varphi_{k-1,i}$ for $i = 1, \ldots, m_{k-1}$. Using the refinement relation (3.1) and the orthogonality of the $\varphi_{k-1,i}$ with $\psi_{k-1,j}$, we get

$$P_k^T G_k a_k = G_{k-1} a_{k-1},$$

which gives the formula for a_{k-1}. If we instead take the inner-products with ψ_{k-1}, we get the formula for b_{k-1}. In view of the linear independence of the functions $\varphi_{k,1}, \ldots, \varphi_{k,m_k}$, the reconstruction formula (3.6) follows immediately from (3.5) and the refinement relations. □

§4. Tensor-product decomposition and reconstruction

In this section we discuss decomposition and reconstruction of functions in tensor product spaces $\mathcal{V}_k \times \widetilde{\mathcal{V}}_\ell$, where the $\mathcal{V}_k$ are as in the previous section, and where $\widetilde{\mathcal{V}}_\ell$ are similar subspaces of an inner-product space $\widetilde{X}$. In particular, suppose

$$\widetilde{\mathcal{V}}_0 \subset \widetilde{\mathcal{V}}_1 \subset \cdots \subset \widetilde{\mathcal{V}}_\ell \subset \cdots,$$

and that

$$\widetilde{\mathcal{V}}_\ell = \widetilde{\mathcal{V}}_{\ell-1} \oplus \widetilde{\mathcal{W}}_{\ell-1}.$$

Let P_k, Q_k, G_k, and H_k be as in the previous section, and let $\widetilde{P}_\ell$, $\widetilde{Q}_\ell$, $\widetilde{G}_\ell$, and $\widetilde{H}_\ell$ be the analogous matrices associated with the spaces $\widetilde{\mathcal{V}}_\ell$.

Theorem 4.1. *Let $f_{k,\ell} = \varphi_k^T A_{k,\ell} \tilde{\varphi}_\ell$ be a function in $\mathcal{V}_k \times \widetilde{\mathcal{V}}_\ell$ associated with a coefficient matrix $A_{k,\ell}$. Then $f_{k,\ell}$ has the orthogonal decomposition*

$$f_{k,\ell} = f_{k-1,\ell-1} + g^{(1)}_{k-1,\ell-1} + g^{(2)}_{k-1,\ell-1} + g^{(3)}_{k-1,\ell-1}, \tag{4.1}$$

with

$$\begin{aligned} f_{k-1,\ell-1} &= \varphi_{k-1}^T A_{k-1,\ell-1} \tilde{\varphi}_{\ell-1} \in \mathcal{V}_{k-1} \times \widetilde{\mathcal{V}}_{\ell-1} \\ g^{(1)}_{k-1,\ell-1} &= \varphi_{k-1}^T B^{(1)}_{k-1,\ell-1} \tilde{\psi}_{\ell-1} \in \mathcal{V}_{k-1} \times \widetilde{\mathcal{W}}_{\ell-1} \\ g^{(2)}_{k-1,\ell-1} &= \psi_{k-1}^T B^{(2)}_{k-1,\ell-1} \tilde{\varphi}_{\ell-1} \in \mathcal{W}_{k-1} \times \widetilde{\mathcal{V}}_{\ell-1} \\ g^{(3)}_{k-1,\ell-1} &= \psi_{k-1}^T B^{(3)}_{k-1,\ell-1} \tilde{\psi}_{\ell-1} \in \mathcal{W}_{k-1} \times \widetilde{\mathcal{W}}_{\ell-1}, \end{aligned}$$

where the matrices $A_{k-1,\ell-1}$, $B^{(1)}_{k-1,\ell-1}$, $B^{(2)}_{k-1,\ell-1}$, *and* $B^{(3)}_{k-1,\ell-1}$, *are computed from the system of equations*

$$\begin{aligned} G_{k-1}A_{k-1,\ell-1}\widetilde{G}_{\ell-1} &= P_k^T D_k \widetilde{P}_\ell \\ G_{k-1}B^{(1)}_{k-1,\ell-1}\widetilde{H}_{\ell-1} &= P_k^T D_{k,\ell}\widetilde{Q}_\ell \\ H_{k-1}B^{(2)}_{k-1,\ell-1}\widetilde{G}_{\ell-1} &= Q_k^T D_{k,\ell}\widetilde{P}_\ell \\ H_{k-1}B^{(3)}_{k-1,\ell-1}\widetilde{H}_{\ell-1} &= Q_k^T D_{k,\ell}\widetilde{Q}_\ell \end{aligned} \tag{4.2}$$

with

$$D_{k,\ell} := G_k A_{k,\ell}\widetilde{G}_\ell.$$

Moreover,

$$A_{k,\ell} = P_k A_{k-1,\ell-1}\widetilde{P}_\ell^T + P_k B^{(1)}_{k-1,\ell-1}\widetilde{Q}_\ell^T + Q_k B^{(2)}_{k-1,\ell-1}\widetilde{P}_\ell^T + Q_k B^{(3)}_{k-1,\ell-1}\widetilde{Q}_\ell^T. \tag{4.3}$$

Proof: To find the formula for $A_{k-1,\ell-1}$, we take the inner-product of both sides of (4.1) with $\varphi_{k-1,i}$ for $i = 1,\ldots,m_{k-1}$ and with $\tilde{\varphi}_{\ell-1,j}$ for $j = 1,\ldots,\tilde{m}_{\ell-1}$. The formulae for the $B^{(i)}_{k-1,\ell-1}$ are obtained in a similar way. The reconstruction formula (4.3) follows directly from (4.1) after inserting the refinement relations and using the linear independence of the components of the vectors φ_k and in $\tilde{\varphi}_\ell$. □

Note that computing the matrices $A_{k-1,\ell-1}$ and $B^{(i)}_{k-1,\ell-1}$ in a decomposition step can be done quite efficiently since several matrix products occur more than once, and we need only solve linear systems of equations involving the four matrices G_{k-1}, H_{k-1}, $\widetilde{G}_{\ell-1}$, and $\widetilde{H}_{\ell-1}$. As we shall see below, in our setting the first two of these are banded matrices, and the second two are periodic versions of banded matrices. All of them can be precomputed and stored in compact form.

§5. The decomposition matrices for the polynomial splines

In this section we construct the matrices P_k, Q_k, and G_k needed for the decomposition and reconstruction of quadratic polynomial splines on the closed interval $[-\pi/2, \pi/2]$. Consider the nested sequence of knots

$$-\pi/2 = x_1^k = x_2^k = x_3^k < x_4^k < \cdots < x_{m_k}^k < x_{m_k+1}^k = x_{m_k+2}^k = x_{m_k+3}^k = \pi/2,$$

where

$$x_i^k = -\pi/2 + (i-3)h_k, \qquad i = 4,\ldots,m_k, \tag{5.1}$$

with $h_k = \pi/(m_k-2)$ and $m_k = 3{\cdot}2^k{+}2$. Let $\{\varphi_{k,i}\}_{i=1}^{m_k}$ be the associated normalized quadratic B-splines with supports on the intervals $[x_i^k, x_{i+3}^k]$, $i = 1,\ldots,m_k$. For each k, the span $\mathcal{V}_k$ of $\varphi_{k,1},\ldots,\varphi_{k,m_k}$ is the m_k dimensional linear space of C^1 quadratic splines with knots at the x_i^k. These spaces are clearly nested. In addition to the well-known *refinement relations*

$$\varphi_{k-1,i} = \frac{(\varphi_{k,2i-3} + 3\varphi_{k,2i-2} + 3\varphi_{k,2i-1} + \varphi_{k,2i})}{4}, \qquad i = 3,\ldots,m_{k-1}-2, \tag{5.2}$$

a simple computation shows that

$$\begin{aligned}
\varphi_{k-1,1} &= (4\varphi_{k,1} + 2\varphi_{k,2})/4 \\
\varphi_{k-1,2} &= (2\varphi_{k,2} + 3\varphi_{k,3} + \varphi_{k,4})/4 \\
\varphi_{k-1,m_{k-1}-1} &= (2\varphi_{k,m_k-1} + 3\varphi_{k,m_k-2} + \varphi_{k,m_k-3})/4 \\
\varphi_{k-1,m_{k-1}} &= (4\varphi_{k,m_k} + 2\varphi_{k,m_k-1})/4.
\end{aligned} \tag{5.3}$$

Equations (5.2), (5.3) provide the entries for the matrix P_k. In particular, the first two and last two columns are determined by (5.3), while for any $3 \leq i \leq m_{k-1} - 2$, the i-th column of P_k contains all zeros except for the four rows $2i-3, \ldots, 2i$ which contain the numbers 1/4, 3/4, 3/4, and 1/4. For example,

$$P_1 = \frac{1}{4}\begin{pmatrix}
4 & 0 & 0 & 0 & 0 \\
2 & 2 & 0 & 0 & 0 \\
0 & 3 & 1 & 0 & 0 \\
0 & 1 & 3 & 0 & 0 \\
0 & 0 & 3 & 1 & 0 \\
0 & 0 & 1 & 3 & 0 \\
0 & 0 & 0 & 2 & 2 \\
0 & 0 & 0 & 0 & 4
\end{pmatrix}.$$

In general, P_k has at most two nonzero entries in each row and and at most four nonzero entries in each column.

In order to construct the matrices Q_k, we now give a basis for the *wavelet space* $\mathcal{W}_{k-1}$. Here we work with the usual L_2 inner-product on $L_2[-\pi/2, \pi/2]$. Let $n_{k-1} = m_k - m_{k-1} = 3 \cdot 2^{k-1}$.

Theorem 5.1. *Given $k \geq 1$, let*

$$\psi_{k-1,1} := \sum_{j=1}^{6} q_{j,1}\varphi_{k,j}$$

$$\psi_{k-1,n_{k-1}} := \sum_{j=1}^{6} q_{j,1}\varphi_{k,m_k-j+1}$$

and for $k \geq 2$, let

$$\psi_{k-1,2} := \sum_{j=2}^{8} q_{j,2}\varphi_{k,j}$$

$$\psi_{k-1,n_{k-1}-1} := \sum_{j=2}^{8} q_{j,2}\varphi_{k,m_k-j+1},$$

where

$$\begin{pmatrix} q_{1,1} \\ q_{2,1} \\ q_{3,1} \\ q_{4,1} \\ q_{5,1} \\ q_{6,1} \end{pmatrix} = \frac{1}{14} \begin{pmatrix} -6864 \\ 8346 \\ -4967 \\ 2083 \\ -406 \\ 14 \end{pmatrix}, \qquad \begin{pmatrix} q_{2,2} \\ q_{3,2} \\ q_{4,2} \\ q_{5,2} \\ q_{6,2} \\ q_{7,2} \\ q_{8,2} \end{pmatrix} = \frac{1}{11} \begin{pmatrix} 780 \\ -1949 \\ 3481 \\ -3362 \\ 1618 \\ -319 \\ 11 \end{pmatrix}. \tag{5.4}$$

In addition, for $k \geq 2$, let

$$\begin{aligned} \psi_{k-1,i} := &-\varphi_{k,2i-3} + 29\varphi_{k,2i-2} - 147\varphi_{k,2i-1} + 303\varphi_{k,2i} - 303\varphi_{k,2i+1} \\ &+ 147\varphi_{k,2i+2} - 29\varphi_{k,2i+3} + \varphi_{k,2i+4}, \end{aligned} \tag{5.5}$$

for $i = 3, \ldots, n_{k-1} - 2$, and set

$$\psi_{0,2} := -\varphi_{1,2} + \frac{5}{2}\varphi_{1,3} - \frac{9}{2}\varphi_{1,4} + \frac{9}{2}\varphi_{1,5} - \frac{5}{2}\varphi_{1,6} + \varphi_{1,7}.$$

Then $\psi_{k-1,1}, \ldots, \psi_{k-1,n_{k-1}}$ form a basis for $\mathcal{W}_{k-1}$.

Proof: The wavelets in (5.5) are just the well-known quadratic spline wavelets, see e.g., [1]. As described in [5], the coefficients of the remaining wavelets can be computed by forcing orthogonality to $\mathcal{V}_{k-1}$. In view of (3.2), the wavelets $\psi_{k-1,1}, \ldots, \psi_{k-1,n_{k-1}}$ are linearly independent if and only if the matrix Q_k is of full rank. This follows since the submatrix of Q_k obtained by taking rows $2, 4, \ldots, 3 \cdot 2^{k-1}$ and $3 \cdot 2^{k-1} + 3, 3 \cdot 2^{k-1} + 5, \ldots, 3 \cdot 2^k + 1$ can easily be seen to be diagonally dominant. For an alternate proof of linear independence, see Lemma 11 of [5]. □

In view of properties of B-splines, it is easy to see that

$$\begin{aligned} \psi_{k-1,i}(\pm\pi/2) &= 0, \qquad i = 2, \ldots, n_{k-1} - 1, \\ D_\theta \psi_{k-1,i}(\pm\pi/2) &= 0, \qquad i = 3, \ldots, n_{k-1} - 2. \end{aligned} \tag{5.6}$$

We now describe the matrices Q_k. By Theorem 5.1,

$$Q_1 = \begin{pmatrix} q_{1,1} & 0 & 0 \\ q_{2,1} & -1 & 0 \\ q_{3,1} & 5/2 & q_{6,1} \\ q_{4,1} & -9/2 & q_{5,1} \\ q_{5,1} & 9/2 & q_{4,1} \\ q_{6,1} & -5/2 & q_{3,1} \\ 0 & 1 & q_{2,1} \\ 0 & 0 & q_{1,1} \end{pmatrix}.$$

and

$$Q_2 = \begin{pmatrix} q_{1,1} & 0 & 0 & 0 & 0 & 0 \\ q_{2,1} & q_{2,2} & 0 & 0 & 0 & 0 \\ q_{3,1} & q_{3,2} & -1 & 0 & 0 & 0 \\ q_{4,1} & q_{4,2} & 29 & 0 & 0 & 0 \\ q_{5,1} & q_{5,2} & -147 & -1 & 0 & 0 \\ q_{6,1} & q_{6,2} & 303 & 29 & 0 & 0 \\ 0 & q_{7,2} & -303 & -147 & q_{8,2} & 0 \\ 0 & q_{8,2} & 147 & 303 & q_{7,2} & 0 \\ 0 & 0 & -29 & -303 & q_{6,2} & q_{6,1} \\ 0 & 0 & 1 & 147 & q_{5,2} & q_{5,1} \\ 0 & 0 & 0 & -29 & q_{4,2} & q_{4,1} \\ 0 & 0 & 0 & 1 & q_{3,2} & q_{3,1} \\ 0 & 0 & 0 & 0 & q_{2,2} & q_{2,1} \\ 0 & 0 & 0 & 0 & 0 & q_{1,1} \end{pmatrix}.$$

For general $k \geq 2$, the nonzero elements in the third column of Q_k are repeated in columns, $4, \ldots, n_{k-1} - 2$, where in each successive column they are shifted down by two rows. The first two and last two columns of Q_k contain the same nonzero elements as Q_2. Clearly, Q_k has at most 4 nonzero entries in each row and at most 8 nonzero entries in each column.

We now describe the Gram matrices G_k, which in general are symmetric and five-banded. To get G_k, we start with the matrix with $66h_k/120$ on the diagonal, $26h_k/120$ on the first subdiagonal, and $h_k/120$ on the second diagonal. Then replace the entries in the 3×3 submatrices in the upper-left and lower-right corners by

$$UL_k := \frac{h_k}{120} \begin{pmatrix} 24 & 14 & 2 \\ 14 & 40 & 25 \\ 2 & 25 & 66 \end{pmatrix}, \qquad LR_k := \frac{h_k}{120} \begin{pmatrix} 66 & 25 & 2 \\ 25 & 40 & 14 \\ 2 & 14 & 24 \end{pmatrix}.$$

For example,

$$G_0 = \frac{h_0}{120} \begin{pmatrix} 24 & 14 & 2 & 0 & 0 \\ 14 & 40 & 25 & 1 & 0 \\ 2 & 25 & 66 & 25 & 2 \\ 0 & 1 & 25 & 40 & 14 \\ 0 & 0 & 2 & 14 & 24 \end{pmatrix}.$$

and

$$G_1 = \frac{h_1}{120} \begin{pmatrix} 24 & 14 & 2 & 0 & 0 & 0 & 0 & 0 \\ 14 & 40 & 25 & 1 & 0 & 0 & 0 & 0 \\ 2 & 25 & 66 & 26 & 1 & 0 & 0 & 0 \\ 0 & 1 & 26 & 66 & 26 & 1 & 0 & 0 \\ 0 & 0 & 1 & 26 & 66 & 26 & 1 & 0 \\ 0 & 0 & 0 & 1 & 26 & 66 & 25 & 2 \\ 0 & 0 & 0 & 0 & 1 & 25 & 40 & 14 \\ 0 & 0 & 0 & 0 & 0 & 2 & 14 & 24 \end{pmatrix}.$$

§6. The decomposition matrices for the trigonometric splines

In this section we present the matrices $\widetilde{P}_\ell$, $\widetilde{Q}_\ell$, and $\widetilde{G}_\ell$ needed for the decomposition and reconstruction of periodic trigonometric splines of order 3. Suppose $\ell \geq 1$, and that

$$\tilde{x}_i^\ell = (i-1)\tilde{h}_\ell, \qquad i = 1, \ldots, \widetilde{m}_\ell + 3, \tag{6.1}$$

is a nested sequence of knots, where $\tilde{h}_\ell = 2^{(1-\ell)}\pi/3$ and $\widetilde{m}_\ell = 3 \cdot 2^\ell$. Let

$$M_{\ell,i}(\phi) := T_{\tilde{h}_\ell}(\phi - \tilde{x}_i^\ell),$$

where

$$T_h(\phi) := \begin{cases} \frac{\sin(\phi/2)^2}{\sin(h/2)\sin(h)}, & 0 \leq \phi \leq h \\ \frac{1}{\cos(h/2)} - \frac{\sin((\phi-h)/2)^2 + \sin((2h-\phi)/2)^2}{\sin(h/2)\sin(h)}, & h \leq \phi \leq 2h \\ \frac{\sin((3h-\phi)/2)^2}{\sin(h/2)\sin(h)}, & 2h \leq \phi \leq 3h \\ 0, & \text{otherwise.} \end{cases} \tag{6.2}$$

is the usual trigonometric B-spline of order three associated with uniformly spaced knots $(0, h, 2h, 3h)$. Set

$$\tilde{\varphi}_{\ell,i}(\phi) = \begin{cases} M_{\ell,i}(\phi), & i = 1, \ldots, \widetilde{m}_\ell - 2, \\ M_{\ell,i}(\phi) + M_{\ell,i}(\phi - 2\pi), & i = \widetilde{m}_\ell - 1, \widetilde{m}_\ell. \end{cases}$$

For later use we define $\tilde{\varphi}_{\ell,\widetilde{m}_\ell+i} = \tilde{\varphi}_{\ell,i}$ for $i = 1, \ldots, 6$.

The span $\widetilde{\mathcal{V}}_\ell$ of $\tilde{\varphi}_{\ell,1}, \ldots, \tilde{\varphi}_{\ell,\widetilde{m}_\ell}$ is the space of periodic trigonometric splines of order three. Clearly, these spaces are nested, and in fact we have the following *refinement relation*:

Theorem 6.1. *For all $\ell \geq 1$ and $1 \leq i \leq \tilde{m}_{\ell-1}$,*

$$\tilde{\varphi}_{\ell-1,i} = u(\tilde{h}_\ell)\tilde{\varphi}_{\ell,2i-1} + v(\tilde{h}_\ell)\tilde{\varphi}_{\ell,2i} + v(\tilde{h}_\ell)\tilde{\varphi}_{\ell,2i+1} + u(\tilde{h}_\ell)\tilde{\varphi}_{\ell,2i+2}, \tag{6.3}$$

where

$$u(h) := \frac{1}{4\cos(h/2)\cos(h)} \qquad v(h) := \frac{\cos(h/2)}{\cos(h)} - u(h).$$

Proof: By nestedness and the nature of the support of T_h,

$$T_{2h}(\phi) = u(h)T_h(\phi) + v(h)T_h(\phi - h) + w(h)T_h(\phi - 2h) + z(h)T_h(\phi - 3h)$$

for some numbers u, v, w, z. By symmetry, it is enough to compute u and v. To find u, we note that on $[0, h]$,

$$T_{2h}(\phi) = u(h)T_h(\phi).$$

Then using (6.2) we can solve for u. To find v we note that

$$T_{2h}(2h) = u(h)T_h(2h) + v(h)T_h(h),$$

and then solve for v using (6.2). □

Theorem 6.1 can now be used to find the entries in the matrix $\widetilde{P}_\ell$ needed in Sect. 2. In particular, each column has exactly the four nonzero elements $u(\tilde{h}_\ell), v(\tilde{h}_\ell), v(\tilde{h}_\ell), u(\tilde{h}_\ell)$, starting in the first row in column one, and shifted down by two rows each time we move one column to the right (where in the last column the last two elements are moved to the top of the column). For example,

$$\widetilde{P}_1 := \begin{pmatrix} u(\tilde{h}_1) & 0 & v(\tilde{h}_1) \\ v(\tilde{h}_1) & 0 & u(\tilde{h}_1) \\ v(\tilde{h}_1) & u(\tilde{h}_1) & 0 \\ u(\tilde{h}_1) & v(\tilde{h}_1) & 0 \\ 0 & v(\tilde{h}_1) & u(\tilde{h}_1) \\ 0 & u(\tilde{h}_1) & v(\tilde{h}_1) \end{pmatrix}.$$

Next we describe a basis for the *wavelet space* $\widetilde{\mathcal{W}}_{\ell-1}$ which has dimension $\tilde{n}_{\ell-1} = 3 \cdot 2^{\ell-1}$ for $\ell \geq 1$. In this case we work with the usual L_2 inner-product on $[0, 2\pi]$.

Theorem 6.2. *Given $\ell \geq 1$, let*

$$\tilde{\psi}_{\ell-1,i} = \sum_{j=0}^{7} \tilde{q}_j(\tilde{h}_\ell)\tilde{\varphi}_{\ell,2i+j-1}, \quad i = 1, \ldots, \tilde{n}_{\ell-1}, \tag{6.4}$$

where

$$\begin{aligned}
\tilde{q}_0(h) &= 1 \\
\tilde{q}_1(h) &= \frac{-h + 5h\cos(h) - h\cos(2h) - 3\sin(h)}{D(h)} \\
\tilde{q}_2(h) &= \frac{3h - 7h\cos(h) - 5h\cos(2h) + 3\sin(3h)}{D(h)} \\
\tilde{q}_3(h) &= \frac{-2h - 7h\cos(h) + 4h\cos(2h) - 4h\cos(3h) + 3\sin(3h)}{D(h)}
\end{aligned}$$

and

$$\tilde{q}_{7-j}(h) = -\tilde{q}_j(h), \qquad j = 0, \ldots, 3,$$

with

$$D(h) := 2h + h\cos(h) - 3\sin(h).$$

Then $\tilde{\psi}_{\ell-1,1}, \ldots, \tilde{\psi}_{\ell-1,\tilde{n}_{\ell-1}}$ is a basis for the space $\widetilde{\mathcal{W}}_{\ell-1}$.

Proof: To construct wavelets in $\widetilde{\mathcal{W}}_{\ell-1}$, we apply Theorem 5.1 of [6] which gives explicit formulae for the $\tilde{q}_i$ in terms of inner-products of $\tilde{\varphi}_{\ell,i}$ with $\tilde{\varphi}_{\ell-1,j}$. To show

that $\tilde{\psi}_{\ell-1,1}, \ldots, \tilde{\psi}_{\ell-1,\tilde{n}_{\ell-1}}$ are linearly independent, it suffices to show that $\widetilde{Q}_\ell$ is of full rank. To see this, we construct a $\tilde{n}_{\ell-1} \times \tilde{n}_{\ell-1}$ matrix B_ℓ by moving the last column of $\widetilde{Q}_\ell$ in front of the first column, and then selecting rows $2, 4, \ldots, \widetilde{m}_\ell$. We now show that this matrix is strictly diagonally dominant, and thus of full rank.

First, we note that in each row of B_ℓ the element on the diagonal is $\tilde{q}_3(\tilde{h}_\ell)$ while the sum of the absolute values of the off diagonal elements is $|\tilde{q}_1(\tilde{h}_\ell)| + |\tilde{q}_5(\tilde{h}_\ell)| + |\tilde{q}_7(\tilde{h}_\ell)|$. A simple computation shows that each of the functions $D(h)$ and $r_i(h) := \tilde{q}_i(h)D(h)$ has a Taylor expansion which is an alternating series. In particular, using the first two terms of each series, we get

$$\begin{aligned} D(h) &> h^5[1/60 - h^2/1260] > 0, \\ r_1(h) &< h^5[-29/60 + 26h^2/315] < 0, \\ r_2(h) &> h^5[49/20 - 89h^2/105] > 0, \\ r_3(h) &< h^5[-101/20 + 1009h^2/420] < 0 \end{aligned}$$

for $0 \le h \le \pi/3 = \tilde{h}_1$. Now it is easy to see that

$$a(h) := \big[|\tilde{q}_3(h)| - |\tilde{q}_1(h)| - |\tilde{q}_5(h)| - |\tilde{q}_7(h)|\big] D(h) = -r_3(h) - r_2(h) + r_1(h) - D(h)$$

also has an alternating series expansion, and we get

$$a(h) > h^5[71/10 - 103h^2/70] > 0$$

for the same range of h. This shows that B_ℓ is strictly diagonally dominant, and the proof is complete. □

The formulae for the $\tilde{q}_i$ in Theorem 6.2 are not appropriate for small values of $\tilde{h}_{\ell-1}$. In this case we can use the following Taylor expansions:

$$\begin{aligned} \tilde{q}_0(h) &= 1 \\ \tilde{q}_1(h) &= -29 + \frac{25}{7}h^2 - \frac{103}{588}\,h^4 + \frac{1255}{271656}\,h^6 + \cdots \\ \tilde{q}_2(h) &= 147 - \frac{307}{7}\,h^2 + \frac{3301}{588}\,h^4 - \frac{545273}{1358280}\,h^6 + \cdots \\ \tilde{q}_3(h) &= -303 + \frac{908}{7}\,h^2 - \frac{3131}{147}\,h^4 + \frac{642583}{339570}\,h^6 + \cdots \end{aligned}$$

Rather than computing them each time we need them, we can precompute and store the necessary values of $\tilde{q}_1(\tilde{h}_\ell)$, $\tilde{q}_2(\tilde{h}_\ell)$, and $\tilde{q}_3(\tilde{h}_\ell)$ for various levels ℓ, see Table 1 in Sect. 7. We can now describe the matrix $\widetilde{Q}_\ell$ needed in Sect. 2 for

decomposing and reconstructing with trigonometric splines. For $\ell = 1$ we have

$$\widetilde{Q}_1 = \begin{pmatrix} \tilde{q}_0 + \tilde{q}_6 & \tilde{q}_4 & \tilde{q}_2 \\ \tilde{q}_1 + \tilde{q}_7 & \tilde{q}_5 & \tilde{q}_3 \\ \tilde{q}_2 & \tilde{q}_0 + \tilde{q}_6 & \tilde{q}_4 \\ \tilde{q}_3 & \tilde{q}_1 + \tilde{q}_7 & \tilde{q}_5 \\ \tilde{q}_4 & \tilde{q}_2 & \tilde{q}_0 + \tilde{q}_6 \\ \tilde{q}_5 & \tilde{q}_3 & \tilde{q}_1 + \tilde{q}_7 \end{pmatrix},$$

where all $\tilde{q}_i$ are evaluated at $\tilde{h}_1$. For $\ell \geq 2$, each column of $\widetilde{Q}_\ell$ contains the 8 entries $\tilde{q}_0, \tilde{q}_1, \tilde{q}_2, \tilde{q}_3, \tilde{q}_4, \tilde{q}_5, \tilde{q}_6, \tilde{q}_7$, evaluated at $\tilde{h}_\ell$. In particular, these entries start in row 1 in column 1, and are shifted down by two each time we move one column to the right (where in the last three columns, entries falling below the last row are moved to the top). Clearly, $\widetilde{Q}_\ell$ has exactly four nonzero entries in each row. For example,

$$\widetilde{Q}_2 = \begin{pmatrix} \tilde{q}_0 & 0 & 0 & \tilde{q}_6 & \tilde{q}_4 & \tilde{q}_2 \\ \tilde{q}_1 & 0 & 0 & \tilde{q}_7 & \tilde{q}_5 & \tilde{q}_3 \\ \tilde{q}_2 & \tilde{q}_0 & 0 & 0 & \tilde{q}_6 & \tilde{q}_4 \\ \tilde{q}_3 & \tilde{q}_1 & 0 & 0 & \tilde{q}_7 & \tilde{q}_5 \\ \tilde{q}_4 & \tilde{q}_2 & \tilde{q}_0 & 0 & 0 & \tilde{q}_6 \\ \tilde{q}_5 & \tilde{q}_3 & \tilde{q}_1 & 0 & 0 & \tilde{q}_7 \\ \tilde{q}_6 & \tilde{q}_4 & \tilde{q}_2 & \tilde{q}_0 & 0 & 0 \\ \tilde{q}_7 & \tilde{q}_5 & \tilde{q}_3 & \tilde{q}_1 & 0 & 0 \\ 0 & \tilde{q}_6 & \tilde{q}_4 & \tilde{q}_2 & \tilde{q}_0 & 0 \\ 0 & \tilde{q}_7 & \tilde{q}_5 & \tilde{q}_3 & \tilde{q}_1 & 0 \\ 0 & 0 & \tilde{q}_6 & \tilde{q}_4 & \tilde{q}_2 & \tilde{q}_0 \\ 0 & 0 & \tilde{q}_7 & \tilde{q}_5 & \tilde{q}_3 & \tilde{q}_1 \end{pmatrix},$$

where all $\tilde{q}_i$ are evaluated at $\tilde{h}_2$.

Finally, we describe the Gram matrices.

Theorem 6.3. *For $\ell \geq 1$, the $3 \cdot 2^\ell \times 3 \cdot 2^\ell$ Gram matrix $\widetilde{G}_\ell$ associated with the $\tilde{\varphi}_{\ell,i}$ is given by*

$$\widetilde{G}_\ell := \begin{pmatrix} I_{00} & I_{01} & I_{02} & 0 & \cdots & 0 & I_{02} & I_{01} \\ I_{01} & I_{00} & I_{01} & I_{02} & 0 & \cdots & 0 & I_{02} \\ I_{02} & I_{01} & I_{00} & I_{01} & I_{02} & \cdots & 0 & 0 \\ & \ddots & & \ddots & & \ddots & & \\ & & \ddots & & \ddots & & \ddots & \\ 0 & 0 & \cdots & I_{02} & I_{01} & I_{00} & I_{01} & I_{02} \\ I_{02} & 0 & \cdots & 0 & I_{02} & I_{01} & I_{00} & I_{01} \\ I_{01} & I_{02} & 0 & \cdots & 0 & I_{02} & I_{01} & I_{00} \end{pmatrix}.$$

where

$$I_{02} := \int_{\tilde{x}_i^\ell}^{\tilde{x}_{i+1}^\ell} \tilde{\varphi}_{\ell,i}\,\tilde{\varphi}_{\ell,i-2} = \gamma_\ell[4\tilde{h}_\ell + 2\tilde{h}_\ell\cos(2\tilde{h}_\ell) - 3\sin(2\tilde{h}_\ell)]$$

$$I_{01} := \int_{\tilde{x}_i^\ell}^{\tilde{x}_{i+2}^\ell} \tilde{\varphi}_{\ell,i}\,\tilde{\varphi}_{\ell,i-1} = \gamma_\ell[-4\tilde{h}_\ell - 20\tilde{h}_\ell\cos(2\tilde{h}_\ell) + 6\sin(2\tilde{h}_\ell) + 3\sin(4\tilde{h}_\ell)]$$

$$I_{00} := \int_{\tilde{x}_i^\ell}^{\tilde{x}_{i+3}^\ell} \tilde{\varphi}_{\ell,i}^2 = \gamma_\ell[4\tilde{h}_\ell\cos(2\tilde{h}_\ell) + 8\tilde{h}_\ell\cos(4\tilde{h}_\ell) + 24\tilde{h}_\ell - 6\sin(2\tilde{h}_\ell) - 6\sin(4\tilde{h}_\ell))]$$

with

$$\gamma_\ell := \frac{1}{64\sin(\tilde{h}_\ell)^4\cos(\tilde{h}_\ell)^2}.$$

Moreover,

$$\widetilde{G}_0 := \begin{pmatrix} I_{00} & I_{01}+I_{02} & I_{01}+I_{02} \\ I_{01}+I_{02} & I_{00} & I_{01}+I_{02} \\ I_{01}+I_{02} & I_{01}+I_{02} & I_{00} \end{pmatrix}.$$

Proof: Using (6.2), the necessary integrals can be computed directly. □

The formulae in Theorem 6.3 are clearly not appropriate for small values of $\tilde{h}_\ell$, in which case the following formulae can be used:

$$I_{02} = \frac{\tilde{h}_\ell}{120}\big[1 + \frac{31}{21}\tilde{h}_\ell^2 + \frac{134}{105}\tilde{h}_\ell^4 + \frac{2971}{3465}\tilde{h}_\ell^6 + \cdots\big]$$

$$I_{01} = \frac{13\tilde{h}_\ell}{60}\big[1 + \frac{295}{273}\tilde{h}_\ell^2 + \frac{146}{195}\tilde{h}_\ell^4 + \frac{299}{693}\tilde{h}_\ell^6 + \cdots\big]$$

$$I_{00} = \frac{11\tilde{h}_\ell}{20}\big[1 + \frac{71}{77}\tilde{h}_\ell^2 + \frac{674}{1155}\tilde{h}_\ell^4 + \frac{12233}{38115}\tilde{h}_\ell^6 + \cdots\big].$$

We can precompute and store the values of I_{00}, I_{01}, and I_{02} for various levels ℓ, see Table 2 in Sect. 7 for the values up to $\ell = 12$.

§7. Implementation

7.1. Decomposition

The decomposition procedure begins with a tensor spline of the form (1.1) based on polynomial splines $\varphi_{k,i}(\theta)$ at a given level $k \geq 1$ and periodic trigonometric splines $\tilde{\varphi}_{\ell,j}(\phi)$ at a given level $\ell \geq 1$ with coefficient matrix $C := A_{k,\ell}$ of size $m_k \times \widetilde{m}_\ell$. To carry out one step of the decomposition, we solve the systems (4.2) for $A_{k-1,\ell-1}$, $B^{(1)}_{k-1,\ell-1}$, $B^{(2)}_{k-1,\ell-1}$, $B^{(3)}_{k-1,\ell-1}$, and set

$$C = \begin{pmatrix} A_{k-1,\ell-1} & B^{(1)}_{k-1,\ell-1} \\ B^{(2)}_{k-1,\ell-1} & B^{(3)}_{k-1,\ell-1} \end{pmatrix}.$$

To continue the decomposition, we now carry out the same procedure on the matrix $A_{k-1,\ell-1}$. This process can be repeated at most $\min(k,\ell)-1$ times, where at each step the new spline coefficients and wavelet coefficients are stored in C. Thus, the entire decomposition process requires no additional storage beyond the original coefficient matrix.

Because of the banded nature of the matrices appearing in (4.2), with careful programming and the use of appropriate band matrix solvers, the j-th step of the decomposition can be carried out with $\mathcal{O}(m_{k-j+1}\widetilde{m}_{\ell-j+1})$ operations. To help keep the number of operations as small as possible, we precompute and store the entries of the matrices G_k, H_k, P_k, Q_k and $\widetilde{G}_\ell, \widetilde{H}_\ell, \widetilde{P}_\ell, \widetilde{Q}_\ell$. appearing in (4.2). Table 1 gives the values of $\tilde{q}_1(\tilde{h}_k)$, $\tilde{q}_2(\tilde{h}_\ell)$ and $\tilde{q}_3(\tilde{h}_\ell)$ for $\ell = 1,\ldots,12$ needed for the $\widetilde{Q}_\ell$. Table 2 gives the values of $I_{00}/\tilde{h}_\ell$, $I_{0,1}/\tilde{h}_\ell$ and $I_{02}/\tilde{h}_\ell$ needed for the $\widetilde{G}_\ell$. The matrices H_k are symmetric positive definite and seven-banded, while the $\widetilde{H}_\ell$ are symmetric positive definite periodic seven-banded matrices.

To check the robustness of the decomposition process, we computed the exact condition numbers of the matrices G_k, H_k, $\widetilde{G}_\ell$, and $\widetilde{H}_\ell$ for up to eight levels. None of the condition numbers exceeded 10, and we can conclude that the algorithm is highly robust.

ℓ	$\tilde{q}_1(\tilde{h}_\ell)$	$\tilde{q}_2(\tilde{h}_\ell)$	$\tilde{q}_3(\tilde{h}_\ell)$
1	-25.288158402784911895	105.15263361113964758	-184.01710881949438326
2	-28.033943811096385992	135.39009725820806026	-269.00057271914225083
3	-28.756039535012008061	144.02032194736046124	-294.20897139729685258
4	-28.938855942719881876	146.25016593522229565	-300.78362470238002386
5	-28.984704348047217637	146.81223291013457079	-302.44473588115810747
6	-28.996175484404513950	146.95303891951439472	-302.86111072242944246
7	-28.999043833434183593	146.98825852278080426	-302.96527310098241998
8	-28.999760956004299506	146.99706455524617238	-302.99131798899351388
9	-28.999940238853933503	146.99926613409589417	-302.99782947935722381
10	-28.999985059704287025	146.99981653322924416	-302.99945736872110255
11	-28.999996264925496984	146.99995413328889043	-302.99986434211038783
12	-28.999999066231338323	146.99998853332107132	-302.99996608552322897

Tab. 1. Trigonometric spline wavelet coefficients for various ℓ.

7.2. Thresholding

Typically, in the j-th step of the decomposition, many of the entries in the matrices $B^{(i)}_{k-j,\ell-j}$ of wavelet coefficients will be quite small. Thus, to achieve compression, these can be removed by a thresholding process. In view of (5.6), tangent plane continuity will be maintained at the poles if we retain all coefficients in the first two and last two rows of these matrices. Given ϵ, at the j-th level we remove all other

ℓ	$I_{00}/\tilde{h}_\ell$	$I_{01}/\tilde{h}_\ell$	$I_{02}/\tilde{h}_\ell$
0	2.0000000000000000000	0.9423311143775626914	0.05766888562243730858
1	0.7173865882718287392	0.29529339212946177894	0.012679980401290518133
2	0.5863256235682111689	0.23350674787359713392	0.009228825204542694601
3	0.5587848830466661676,	0.22072647211850900468	0.008547276418657547047
4	0.5521783423263619826	0.21767257645539869275	0.008386225140326574126
5	0.5505434780490859489	0.21691758424366982979	0.008346519562452568337
6	0.5501358004443718685	0.21672936114999970712	0.008336627601639628844
7	0.5500339457967328606	0.21668233810682990252	0.008334156757445556228
8	0.5500084861795729324	0.21667058439043531220	0.008333539180427623907
9	0.5500021215280431720	0.21666764608909212581	0.008333384794548569195
10	0.5500005303809576733	0.21666691152174074237	0.008333346198602246618
11	0.5500001325951735985	0.21666672788040191760	0.008333336549648380680
12	0.5500000331487892859	0.21666668197009840015	0.008333334137411958859

Tab. 2. Inner products of Trigonometric B-splines for various ℓ.

wavelet coefficients in $B^{(1)}_{k-j,\ell-j}$ and $B^{(2)}_{k-j,\ell-j}$ whose absolute values are smaller than $\epsilon/2^j$. We do the same for $B^{(3)}_{k-j,\ell-j}$ using a threshold value of $\epsilon/(300\cdot 2^j)$. This smaller threshold is applied because of the scaling of the wavelets.

7.3. Reconstruction

In view of (4.3), to carry out one reconstruction step simply involves matrix multiplication using our stored matrices. Because of the band nature of these matrices, the computation of $A_{k-j,\ell-j}$ requires $\mathcal{O}(m_{k-j}\widetilde{m}_{\ell-j})$ operations. At each step of the reconstruction we can store these coefficients in the same matrix C where the decomposition was carried out.

§8. Examples

To test the general performance of the algorithms, we begin with the following simple example.

Example 1. Let $k = 8$ and $\ell = 9$, and let s be the tensor spline with coefficients

$$c_{ij} = \cos((\tilde{x}^9_{j+2} - \tilde{x}^9_{j+1})/2), \qquad i = 1,\ldots,m_8, \quad j = 1,\ldots,\widetilde{m}_9.$$

Discussion: Since the normalized quadratic B-splines form a partition of unity, it follows from (2.1) that with these coefficients, $s \equiv 1$ for all $(\theta,\phi) \in H$, *i.e.*, the corresponding surface is exactly the unit sphere. In this case the coefficient matrix is of size 770×1536, and involves 1,182,720 coefficients. To test the algorithms, we performed decomposition with various values of ϵ, including zero. In all cases, after reconstruction we got coefficients which were correct to machine accuracy (working

in double precision). The run time on a typical workstation is just a few seconds for a full 7 levels of decomposition and reconstruction. □

The illustrate the ability of our multiresolution approach to achieve high levels of compression while retaining important features of a surface, we now create a tensor spline fit to a smooth surface with a number of bumps.

Example 2. Let $\mathcal{B}$ be the surface shown in the upper left-hand corner of Figure 1.

Discussion: The surface $\mathcal{B}$ was created by fitting a spline $f_{8,8}$ to data created by choosing 10 random sized subrectangles at random positions in H, and adding tensor product quadratic B-splines of maximum height 3/4 with support on each such rectangle to the constant values corresponding to the unit sphere. For $k = \ell = 8$, the coefficient matrix is of size 770×768 and involves 591,360 coefficients. To test the algorithms, we performed decomposition with the thresholding values $\epsilon_r = 10^{-r}$ for $r = 1, \ldots, 9$. Table 3 shows the results of a typical run with $\epsilon = .0001$.

step	nco
0	591360
1	152064
2	43150
3	16649
4	10720
5	9772
6	9746
7	9745

Tab. 3. Reduction in coefficients in Example 2 with $\epsilon = .0001$.

Almost 3/4 of the coefficients are removed in the first step of decomposition, and after 7 steps we end up with only 9745 coefficients (which amounts to a 60:1 compression ratio). Table 4 shows the differences between the original coefficients and the coefficients obtained after reconstruction. The table lists both the maximum norm

$$e_\infty := \max_{ij} |c_{ij} - \tilde{c}_{ij}|,$$

and the average ℓ_1 norm

$$e_1 := \frac{\sum_{ij} |c_{ij} - \tilde{c}_{ij}|}{m\widetilde{m}},$$

where c_{ij} are the original coefficients, and $\tilde{c}_{ij}$ are the reconstructed ones. Due to the scaling of the wavelets these numbers are somewhat larger than the corresponding ϵ.

The surfaces corresponding to the values $\epsilon = 0, 10^{-4}, 10^{-3}, 10^{-2}$ are shown in Figure 1. At $\epsilon = .0001$ we get near perfect looking reconstruction, while at $\epsilon = .001$ the major features are reproduced with only small wiggles in the surface. At $\epsilon = .01$

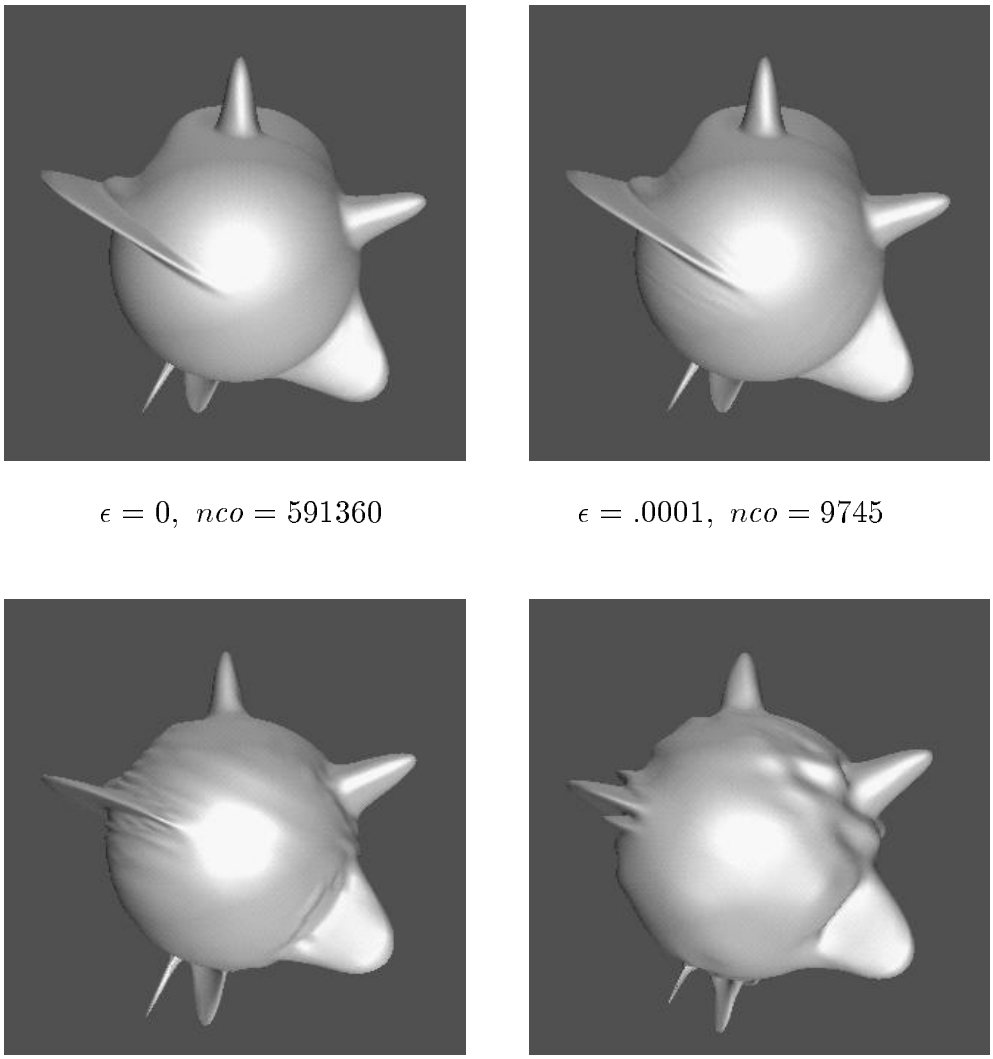

$\epsilon = 0,\ nco = 591360$ $\epsilon = .0001,\ nco = 9745$

$\epsilon = .001,\ nco = 8276$ $\epsilon = .01,\ nco = 7668$

Fig. 1. Compressed surfaces for Example 2.

we have larger oscillations in the surface. This example shows that there is a critical value of ϵ beyond which the surface exhibits increasing oscillations with very little additional compression. □

§9. Remarks

Remark 9.1. The approach discussed in this paper was first presented at the Taormina Wavelet Conference in October of 1993, and as far as we know was the first spherical multiresolution method to be proposed. The corresponding proceedings paper [6] focuses on the general theory of L-spline wavelets, and due to space limitations, a full description of the method could not be included. In the meantime

ϵ	nco	e_∞	e_1
0	591360	0	0
10 (-9)	110365	5.54 (-7)	2.73 (-8)
10 (-8)	73928	6.93 (-6)	2.33 (-7)
10 (-7)	44304	5.79 (-5)	1.81 (-6)
10 (-6)	24414	3.74 (-4)	1.39 (-5)
10 (-5)	13800	3.10 (-3)	8.00 (-5)
10 (-4)	9745	1.39 (-2)	4.70 (-4)
10 (-3)	8276	5.69 (-2)	2.83 (-3)
10 (-2)	7740	2.69 (-1)	1.51 (-2)
10 (-1)	7668	6.02 (-1)	3.24 (-2)

Tab. 4. Coefficient errors in Example 2 for selected ϵ.

we have become aware of the recent work [2,4,8,9,13]. In [2] the authors use tensor splines based on exponential splines in the ϕ variable. The method in [4] uses discretizations of certain continuous wavelet transforms based on singular integral operators, while the method in [8] uses tensor functions based on polynomials and trigonometric polynomials. Finally, the method in [9] utilizes C^0 piecewise linear functions defined on spherical triangulations. Except for the last method, we are not aware of implementations of the other methods.

Remark 9.2. In our original paper [6], an alternative way of making sure that tangent plane continuity is maintained at the poles was proposed. The idea is to decompose the original tensor product function s into two parts s_H and s_P, where

$$s_H := \sum_{i=3}^{m_k-2} \sum_{j=1}^{\widetilde{m}_\ell} c_{ij} \varphi_{k,i} \tilde{\varphi}_{\ell,j}$$

and $s_P := s - s_H$. Then decomposition, threshnolding, and reconstruction can be performed on s_H. After adding s_P, the reconstructed spline possesses tangent plane continuity at the poles. Our implementation of this method exhibits essentially the same performance in terms of compression and accuracy as the method described here, but for higher compression ratios produces surfaces which are not quite as visually pleasing near the poles.

Remark 9.3. The method described here can be extended to the case of nonuniform knots in both the θ and ϕ variables. In this case the computational effort increases considerably since the various matrices can no longer be precomputed and stored.

Remark 9.4. In Sect. 4 we have presented the details of the tensor-product decomposition and reconstruction algorithms assuming that the initial function $f_{k,\ell}$ lies in the space $\mathcal{V}_k \oplus \widetilde{\mathcal{V}}_\ell$, with k and ℓ not necessarily the same. Since these spaces can always be reindexed, this is not strictly necessary in the abstract setting, but was convenient for our application where there is a natural indexing for our spaces.

Remark 9.5. In computing the coefficients needed in Sections 5 and 6, we found it convenient to use Mathematica.

Remark 9.6. There are several methods for computing approximations of the form (1.1). An explicit quasi-interpolation method using data on a regular grid (along with derivatives at the north and south poles) can be found in [11]. The same paper also describes a two-stage method which can be used to interpolate scattered data, and a least squares method which can be used to fit noisy data. A general theory of quasi-interpolation operators based on trigonometric splines can be found in [7].

Remark 9.7. A closed, bounded, connected set U in $\mathbb{R}^3$ which is topologically equivalent to a sphere is called a *sphere-like surface*. This means that there exists a one-to-one mapping of U onto the unit sphere S. Moreover, there exists a point O inside the volume surrounded by U, such that every point on the surface U can be seen from O. Such surfaces are also called *starlike*. For applications, we can focus on the class of sphere-like surfaces of the form

$$U = \{v\rho(v) : \ v \in S\},$$

where ρ is a smooth function defined on S. Then each function f defined on U is just the composition $f(\cdot) = g(\rho(\cdot))$ with ρ of a function g defined on S.

Remark 9.8. As indicated in [9], compression methods on the sphere can be adapted to the problem of creating multiresolution representations of *bidirectional reflection distribution functions* (BRDF's), althought the basic domain for such functions is actually a hemisphere. We will explore the use of our method for this purpose in a later paper.

Remark 9.9. It is well-known that the polynomial B-splines are stable. In particular for quadratic B-splines (φ_i) with general knots

$$\frac{1}{3}\|c\|_\infty \le \|\sum c_i\varphi_i\|_{L_\infty} \le \|c\|_\infty$$

for all coefficient vectors c. The same bounds hold for trigonometric splines since the linear functionals

$$\lambda_i f := [-f(\tilde{x}_{i+1}) + 2(1+\sigma_i)f\Big(\frac{\tilde{x}_{i+1}+\tilde{x}_{i+2}}{2}\Big) - f(\tilde{x}_{i+2})]/2$$

introduced in [11] are dual to the $\tilde{\varphi}_i$, *i.e.*,

$$\lambda_i\tilde{\varphi}_j = \delta_{ij}, \qquad i,j = 1,\dots,\widetilde{m},$$

where $\sigma_i := \cos((\tilde{x}_{i+2}) - \tilde{x}_{i+1})/2)$. Analogous stability results hold for general p-norms.

References

1. Chui, C. K., *An Introduction to Wavelets*, Academic Press, Boston, 1992.
2. Dahlke, S., W. Dahmen, I. Weinreich, and E. Schmitt, Multiresolution analysis and wavelets on S^2 and S^3, Numer. Funct. Anal. Optimiz. **16** (1995), 19-41.
3. Dierckx, P., Algorithms for smoothing data on the sphere with tensor product splines, Computing **32** (1984), 319–342.
4. Freeden, W. and U. Windheuser, Spherical wavelet transform and its discretization, Adv. Comp. Math. **5** (1996), 51–94.
5. Lyche, T. and K. Mørken, Spline-wavelets of minimal support, in *Numerical Methods in Approximation Theory*, D. Braess and L. L. Schumaker (eds.), Birkhäuser (Basel), 1992, 177–194.
6. Lyche, T. and L. Schumaker, L-spline wavelets, in *Wavelets: Theory, Algorithms, and Applications*, C. Chui, L. Montefusco, and L. Puccio (eds.), Academic Press (New York), 1994, 197–212.
7. Lyche, T., L. Schumaker, and S. Stanley, Quasi-interpolants based on trigonometric splines, J. Approx. Theory, to appear.
8. Potts, D., and M. Tasche, M., Interpolatory wavelets on the sphere, in *Approximation Theory VIII, Vol. 2: Wavelets*, Charles K. Chui and Larry L. Schumaker (eds.), World Scientific Publishing Co., Inc. (Singapore), 1995, 335–342.
9. Schröder, P. and W. Sweldens, Spherical wavelets: efficiently representing functions on the sphere, in *Computer Graphics Proceedings, Annual Conference Series*, 1995, ACM SIGGRAPH, 161–172.
10. Schumaker, L. L., *Spline Functions: Basic Theory*, Wiley, New York, 1981.
11. Schumaker, L. L. and C. Traas, Fitting scattered data on spherelike surfaces using tensor products of trigonometric and polynomial splines, Numer. Math. **60** (1991), 133–144.
12. Stollnitz, E., T. DeRose, and D. Salesin, *Wavelets for Computer Graphics*, Morgan Kaufmann, San Francisco, 1996.
13. Weinreich, I., Biorthogonale Wavelets auf der Sphäre, dissertation, Tech. Univ. Aachen, 1997.